Theor Chem Acc (2009) 123:75–84
DOI 10.1007/s00214-009-0539-7

REGULAR ARTICLE

The role of amide ligands in the stabilization of Pd(II) tricoordinated complexes: is the Pd–NR_2 bond order single or higher?

Salvador Moncho · Gregori Ujaque · Pablo Espinet · Feliu Maseras · Agustí Lledós

Received: 11 February 2009 / Accepted: 11 February 2009 / Published online: 6 March 2009

Abstract The existence of tricoordinated Pd(II) complexes has been a matter of controversy for a long time. The recent X-ray characterization of a family of Pd complexes [PdArXL] allowed to certify the existence of true tricoordinated Pd(II) species. The unique role played by the amido ligand (X = NR_2), among a family of X ligands, was noticed in a previous computational work. Here, the influence of the R substituents at the amide and the nature of the Pd–N_{amido} bond are theoretically analyzed. The relative stability of d^8 tricoordinated [PdLAr(NR_2)] complexes versus d^8 tetracoordinated derivatives as a function of the R substituents is studied by analyzing the two most common ways to fill the vacant coordination site in a tricoordinated complex: solvent coordination (with tetrahydrofuran as solvent), or dimerization giving [(μ-NR_2)$_2$ $Pd_2L_2Ar_2$]) complexes. The nature of the Pd–N bonding interaction is analyzed using several theoretical schemes as molecular orbitals, QTAIM, ELF and NBO. Each of these schemes suggests that the order of the Pd–N bond in this family of complexes is higher than one. An asymmetric π interaction between the nitrogen lone pair and the LUMO over the tricoordinated Pd center is proposed as an important source of additional stabilization of tricoordinated species provided by amido ligands.

Keywords Palladium chemistry · Amide ligands · Theoretical transition metal chemistry

Dedicated to Prof. Santiago Olivella on the occasion of his 65th birthday.

S. Moncho · G. Ujaque · F. Maseras · A. Lledós (✉)
Departament de Química, Facultat de Ciències,
Universitat Autònoma de Barcelona,
08193 Bellaterra, Barcelona, Spain
e-mail: agusti@klingon.uab.es

P. Espinet
IU CINQUIMA/Química Inorgánica, Facultad de Ciencias,
Universidad de Valladolid, 47071 Valladolid, Spain

F. Maseras
Institute of Chemical Research of Catalonia (ICIQ),
43007 Tarragona, Spain

1 Introduction

Electronic population on the metallic center of transition metal complexes (both in intermediates and in transition states) is a crucial characteristic for the understanding of their properties and reactivity. Most organometallic complexes in their common oxidation state have a formal 18-electron counting, which is considered the standard rule, but late transition metals show a tendency to 16-electron counting. Thus, for isolated Pd(II) (d^8) complexes the square–planar 4-coordination with a formal 16-electron counting is absolutely dominant, although the less abundant five-coordination is not uncommon [1]. However, three-coordinated palladium(II) complexes are a real rarity hardly expected to be found as stable species, although they are often proposed as feasible intermediate structure in mechanistic proposals [2]. In this respect, theoretical calculations have proved to be highly useful in determining reaction mechanisms in organic [3–5] and organometallic chemistry [6, 7].

One kind of formally three-coordinated Pd(II) complexes frequently depicted as intermediates in very important catalytic cycles has a PdArXL stoichiometry with Ar = aromatic ring, X = anionic ligand, and L = phosphine. In practice, with unexceptional ligands the fourth coordination site is admittedly satisfied either by

coordination of a solvent molecule to give [PdArXL(s)] (if the solvent is coordinating), or by dimerization to give $[(\mu\text{-X})_2Pd_2Ar_2L_2]$ complexes, in the lack of other coordinating molecules or a good coordinating solvent [8]. In both cases the metal center is four-coordinated.

The recent use of hindered ligands (with large steric demand and extraordinary catalytic performance) has led to the preparation of a number of monomeric Pd(II) complexes with only three-coordinated ligands [9–35]. Many of these species have been X-ray characterized, and the three-coordination has turned out to be deceptive: the supposedly empty coordination site is in fact occupied by an agostic interaction to a C–H bond of the ligands making these complexes strictly four-coordinated [36–38]. Similar cases have been found in related isoelectronic complexes of Ni(II) [39], Pt(II) [40–43], and Rh(I) [44, 45]. Very recently, however, Yamashita and Hartwig [46] reported the characterization of a family of related complexes [PdArXL] (Ar = C_6H_4–OMe-*p*; X = NAr'_2, Ar′ = 3,5-$(CF_3)_2C_6H_3$; L = P^tBu_3, FcP^tBu_2, $(Ph_5Fc)P^tBu_2$; Fc = ferrocenyl), that are unambiguously true three-coordinated complexes, with no agostic interaction as the fourth ligand.

Recently, we studied theoretically the relative stability of coordinatively unsaturated tricoordinated PdXArL complexes versus their tetracoordinated counterparts, by considering the energy balance for two practical processes leading from three- to four-coordination: solvent coordination, and dimerization [47]. The influence of the ligands (L = PH_3, PMe_3, PPh_3, P^tBu_3, 1-AdP^tBu_2; Ar = C_6F_5, C_6H_5, C_6H_4OH, $C_6H_4OCH_3$, $C_6H_4NH_2$, $C_6H_2(NH_2)_3$; X = F, Cl, Br, I, OH, SH, NH_2, PH_2, CH_3) on these two processes was systematically considered. This revealed that the three-coordinated Pd(II) species become more accessible for more electron-donating ligands. Nevertheless, the most important stabilizing effect is the hindrance of the ligands, mainly governed by the phosphine ligands. These results help to explain the experimental fact that bulky ligands in transition-metal catalyzed reactions use to be highly active, probably because they facilitate dissociation in critical steps.

The accessibility of three-coordinated [PdArX(PR_3)] species was also affected by the second ligand *cis* to the empty position. In this sense, our energy calculations showed that only NR_2 ligands were able to produce true three-coordinated species energetically stable in front of the four-coordinated alternatives formed by the addition of a solvent molecule or by dimerization. The amido ligand is a very strong σ-donor, which would help to compensate the electron deficiency in a tricoordinated d^8 complex. However, this would hardly be enough to compensate the high electrophilicity of a coordinatively unsaturated Pd(II) center. Looking at some structural features of the complexes, we hypothesized that the striking case of [PdAr(NR_2)(PR_3)] complexes could be generated by some Pd–N double bond character due to π donation of electron N lone pair of the coordinated amido ligand to an "empty" Pd orbital, therefore the amido group acting as a σ-donor, single-face π-donor ligand, as suggested for related cases in other transition metal complexes [2, 48, 49] (Fig. 1). Due to the high interest of the case, a deeper study of the bonding was undertaken.

2 Computational details

Energy and geometry optimizations were performed using the Gaussian03 package [50]. All the geometries were fully optimized using Density Functional Theory with the B3PW91 functional [51, 52]. For the Pd and P atoms the lanl2dz effective core potential was used to describe the inner electrons [53, 54], along with their associated double-ζ basis set for the remaining electrons; an extra series of d-polarization functions was added for P (exponent 0.387) [55]. The rest of the atoms were described with a 6-31G basis, adding an extra d-polarization function in O, N and F atoms, as well as the C atoms [except those in Tetrahydrofuran (THF)]. Frequency analysis was used by us to identify all the optimized structures as minima within the potential energy surface. Single point calculations including solvent effects were performed at the optimized gas-phase geometries (ΔE_{solv}), using the PCM approach [56–59] as implemented in Gaussian03. THF was chosen as solvent ($\varepsilon = 7.58$). ΔE corresponds to the potential energy and ΔG to the Gibbs energy in gas phase. ΔE_{solv} and ΔG_{solv} stand for the potential and Gibbs energies including solvent effects, respectively. The ΔG_{solv} is calculated according to the following formula: $\Delta G_{solv} = \Delta E_{solv} + (\Delta G - \Delta E)$ [60]. The values commented in the text or represented in the figures refer to the values including solvent effects, unless otherwise specified.

The electron density analysis studies were performed from the density obtained with Gaussian03, at the level of calculation used in optimizations. Xaim 1.0 software [61] was used for topological analysis of the electron density by means of the Bader's AIM theory [62, 63] and ToPMoD software package [64] was used to analyze the electron localization function (ELF). NBO calculations were

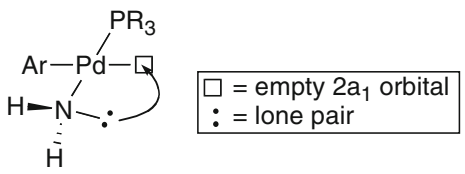

Fig. 1 Sketch of the π donation of the electron lone pair of the amide ligand to the empty Pd orbital

computed with the NBO program [65] as integrated in Gaussian03. Molecular orbitals were drawn using GaussView [66].

3 Results and discussion

3.1 Substituent effects on the NR_2 ligand

3.1.1 Energy stabilization

The stability of a chemical compound has not a single and clear meaning and needs to be referred to particular conditions. We choose to calculate the energy of the three-coordinated complex change associated with the occupation of the vacant site in two different reactions likely to occur in the flask: solvent coordination, represented by coordination of tetrahydrofuran (Eq. 1, s = THF), and dimerization through double bridge formation (Eq. 2). Accordingly, the less negative (or more positive) the energy balance, the higher the relative stability of the tri-coordinated species as compared to its tetracoordinated counterpart.

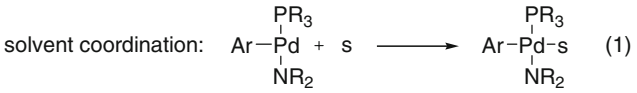

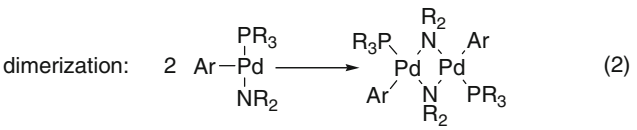

The reaction energies of both processes (solvent coordination and dimerization) were computed for a series of alkyl and aryl amides Table 1). The general trends observed can be compared depending on the alkyl or aryl nature of the amide substituent. For alkyl groups the bigger the substituent the more stable the T-shaped species. Solvent coordination is unfavored for any of the amides considered. The dimerization process, however, is highly affected by the bulkiness of the substituent groups. For NH_2 and NMe_2 the dimerization is favorable, whereas for the rest of amide substituents the three-coordinated species is calculated to be the most stable one. The electron donating capacity of the amido ligand also increases with the size of the substituent for the alkyl group. Thus, both effects, increasing bulkiness along with increasing electron donating ability, should cooperate to stabilize the three-coordinated complexes.

The behavior observed for the aryl amido ligands is different, which is not surprising since these ligands are expectedly less donor than the alkylamido ligands. The checked ligands give negative or just slightly positive ΔG_{solv} values for either solvation or dimerization, therefore suggesting that there is no clear coordination preference with these ligands. Nevertheless, it should be noted that the negative ΔG_{solv} values for dimerization process are rather small (<3.5 kcal/mol) compared to those obtained for the less bulky amido ligands with alkyl substituents (>13.3 kcal/mol) suggesting that the use of bulky phosphines might give rise to stable three-coordinated complexes.

Table 1 Calculated ΔE, ΔE_{solv}, ΔG and ΔG_{solv} (kcal/mol) for the solvent coordination (THF as solvent) and the dimerization processes, varying R in [PdPh(NR2)(PH3)]

NR_2	Solvent coordination				Dimerization			
	ΔE	ΔE_{solv}	ΔG	ΔG_{solv}	ΔE	ΔE_{solv}	ΔG	ΔG_{solv}
NH_2	−14.8	−11.8	−3.0	0.0	−28.6	−26.9	−19.7	−18.0
NMe_2	−11.1	−9.7	1.2	2.7	−22.1	−23.3	−12.2	−13.3
N^nPr_2	−7.9	−5.7	4.9	7.1	−19.7	−4.0	−8.8	6.9
N^iPr_2	−3.9	−4.8	10.0	9.1	−3.1	−6.7	8.4	4.8
N^tBu_2	−3.8	−3.6	8.8	9.0	12.0	7.9	23.8	19.8
NPh_2	−14.7	−12.7	−1.5	0.5	−15.4	−13.4	−5.5	−3.5
$NAr^1{}_2$[a]	−18.9	−15.1	−4.6	−0.8	−14.6	−9.3	−3.7	1.6
$NAr^2{}_2$[b]	−12.0	−9.4	1.2	3.8	−14.6	−12.5	−4.5	−2.4

[a] $Ar^1 = 3,5\text{-}(CF_3)_2C_6H_3$

[b] $Ar^2 = 4\text{-}NH_2C_6H_4$

3.1.2 Geometrical parameters

The optimized structures for the T-shaped complexes [$PdPh(NH_2)(PH_3)$], [$PdPh(N^tBu_2)(PH_3)$], and [$PdPh(NPh_2)(PH_3)$] are shown in Fig. 2. Selected geometrical parameters for all of the calculated structures, including T-shaped and square–planar complexes (the fourth ligand is a THF molecule), are shown in Table 2. We have considered a ligand distribution with the amide group in *cis* position relative to the vacant and the phenyl ring in a *trans* position. Both experimental data and calculations agree with this ligand arrangement corresponding to the most stable tricoordinated isomer [47].

To evaluate the changes in the amido ligand upon coordination of a fourth ligand to the metal center, two main data have been considered: the Pd–N bond length (related to the strength of the metal–ligand interaction), and the N pyramidalization (related to the sp^3 or sp^2 character). The latter can be represented by the sum of the three bond angles around the N atom, which is 360° for a planar amide and decreases with increasing sp^3 character. Pyramidalization is also reflected by the dihedral angles between the substituents, A(R–N–Pd–R), or between them and the aromatic ligand, A(R–N–Pd–C).

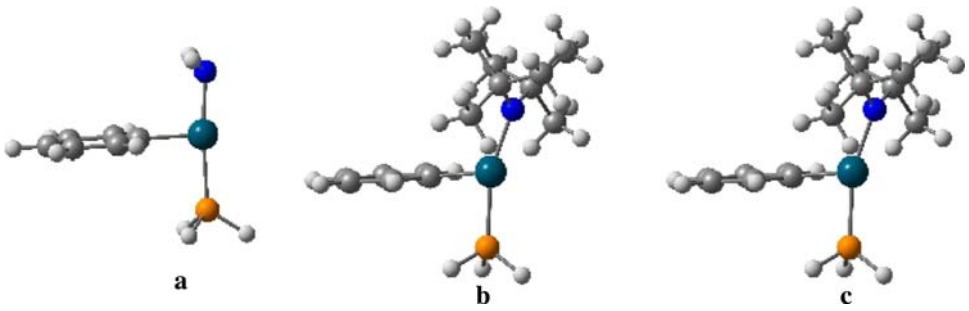

Fig. 2 Optimized geometries for: **a** [PdPh(NH_2)(PH_3)], **b** [PdPh(N^tBu_2)(PH_3)] and **c** [PdPh(NPh_2)(PH_3)]

Table 2 DFT geometrical parameters for different complexes of formula [PdPh(NR_2)(PH_3)] and [PdPh(NR_2)(PH_3)(THF)] varying the R substituent

Amido	Ligands	d(N-Pd) (Å)	Sum (°)	A(RNPdR) (°)	A(RNPdC) (°)	A(NPdP) (°)	A(NpdC) (°)	A(PPdC) (°)	d(OPd) (Å)	d(CPd) (Å)	d(PPd) (Å)
NH_2	3	1.958	333.3	121.0	−60.5/60.5	174.5	95.9	98.7	–	1.998	2.328
NH_2	4	2.025	316.4	109.1	−54.5/54.5	178.2	89.4	88.8	2.300	1.997	2.331
NMe_2	3	1.963	349.5	141.5	−71.0/70.5	171.4	100.1	88.5	–	2.009	2.314
NMe_2	4	2.034	339.9	128.9	−64.9/64.0	179.6	92.2	88.0	2.343	2.002	2.329
N^nPr_2	3	1.969	350.5	143.7	−72.5/71.2	171.6	99.9	83.6	–	2.011	2.313
N^nPr_2	4	2.041	340.7	131.1	−60.1/71.0	179.5	91.9	88.3	2.357	2.004	2.324
N^iPr_2	3	1.975	357.5	160.9	−75.7/85.2	162.4	113.9	83.6	–	2.018	2.291
N^iPr_2	4	2.055	346.2	137.6	−73.8/63.8	174.0	97.6	86.0	2.432	2.013	2.326
N^tBu_2	3	2.002	358.1	164.5	−79.0/85.5	161.7	114.9	83.4	–	2.018	2.287
N^tBu_2	4	2.068	353.3	151.8	−84.1/67.6	174.3	102.0	83.4	2.568	2.011	2.321
NPh_2	3	2.010	354.7	154.1	−73.8/80.3	173.5	98.7	87.8	–	2.010	2.299
NPh_2	4	2.070	359.5	171.8	−102.9/68.9	174.6	92.4	85.6	2.308	2.000	2.297
NAr^{1a}_2	3	2.036	355.0	154.9	−75.6/79.4	176.3	96.7	86.9	–	1.999	2.298
NAr^{1a}_2	4	2.098	359.8	174.6	−110.6/64.0	173.7	90.8	83.9	2.280	1.999	2.288
NAr^{2b}_2	3	2.005	354.4	153.2	−71.5/81.7	171.9	99.6	88.5	–	2.022	2.298
NAr^{2b}_2	4	2.070	359.5	171.78	−102.9/68.9	174.6	92.0	85.6	2.308	2.000	2.297

[a] $Ar^1 = 3,5\text{-}(CF_3)_2C_6H_3$

[b] $Ar^2 = 4\text{-}NH_2C_6H_4$

The general trend in metal–ligand bonding is that the bond distances increase with coordination number. Accordingly T-shaped compounds show shorter Pd–N bond distances than their solvent-coordinated counterparts. For Pd–P bond distances, a similar trend is found, though in a much lesser extent. However, no clear trend is observed for the Pd–C bond distances. This different behavior of the metal–ligand bond lengths (which somehow reflect their strength variations) suggests the predominant role of amide ligand in T-shaped species stabilization.

Depending on the amido substituents (aryl or alkyl), the trends observed for the N pyramidalization are different. The T-shaped complexes present the amido N atom closer to planar for the alkylic substituents, with sum of angles ranging between 349° and 359°. Coordination of a solvent molecule on the vacant site decreases the sum of dihedral angles by approx. 10°. This change may be related to the strength and the nature of the Pd–N bond and how the lone pair interacts with the Pd center. For the case of the amido ligands with arylic substituents the trend is the opposite. The complexes with a coordinated solvent molecule (four-coordinated) show a fully planar structure of the N atom. The three-coordinated species, however, introduces some degree of pyrimidalization on the N atom (the sum of dihedral angles decreases by approx. 5°). This might be interpreted as an indication that the N lone pair is fully delocalized over the aromatic rings of the substituents in the four-coordinated Pd complexes, whereas, when the vacant site is generated, the lone pair is additionally interacting with the metal center, producing some degree of pyramidalization on the N atom.

A typical feature of bonds of order higher than one is that they produce hindrance to rotation. Thus, significantly higher rotation barriers can be expected for double bonds compared to single bonds. In this sense, the rotation barrier of the Pd–N bond was calculated for the simplest model of T-shaped amido complex ($[PdPhNH_2PH_3]$). An energy barrier of 10.3 kcal/mol was obtained for this rotation from the minimum (with a dihedral HNPdC angle of 60.5°) to the TS (with a dihedral HNPdC angle of −106.5°); so there is a 167.0° rotation [67]. Such a high barrier reveals a significant impediment to rotation. This barrier was also calculated for the protonated complex $[PdPhNH_3PH_3]^+$, where the amido ligand has been replaced by ammonia. Coordinated ammonia has no lone pairs left, therefore avoiding any possible extra electron donation to the Pd center. In this case, rotation is an essentially barrierless process (0.04 kcal/mol). Such different values in the rotation energy barrier for coordinated NH_2^- and NH_3 support a much stronger Pd–N interaction in the case of the amido ligand, due to the availability of the lone pair.

3.2 Analysis of the Pd–N_{amido} bond

3.2.1 Molecular orbitals

A qualitative knowledge of the molecular orbitals over the metallic center is useful to understand the behavior of the Pd–N_{amido} interaction. A qualitative scheme of the shapes and energies of the main orbitals around the metal is shown in Fig. 3 for both square–planar and T-shaped ideal complexes [68, 69]. The $d(z^2)$ orbital gets slightly lower in energy in the T-shaped complex, but the most important difference is observed for $d(x^2 - y^2)$ orbital, which undergoes an important stabilization and a marked growing of the lobe oriented towards the vacant site. Pd(II) complexes have a d^8 configuration, therefore this orbital is the main atomic orbital involved in the lowest unoccupied molecular orbital (LUMO).

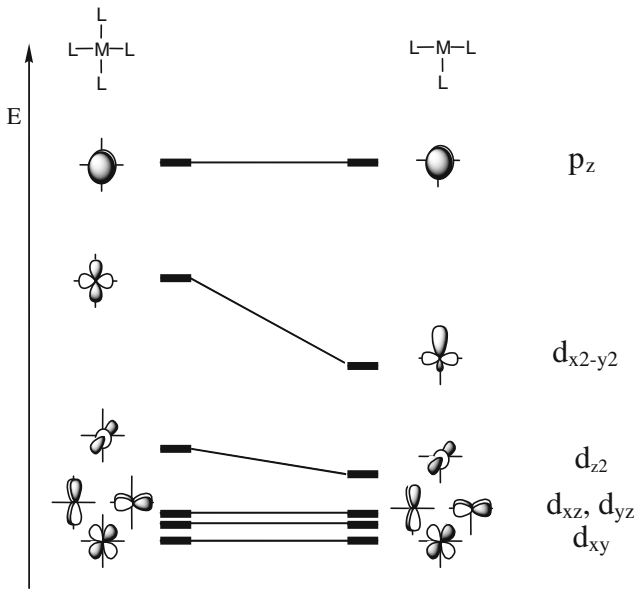

Fig. 3 Sketch of molecular orbitals around the metal center in square–planar ML_4 and T-shaped ML_3 ideal complexes with σ ligands

The asymmetry in the LUMO allows for the formation of an interaction with the lone pair of the N atom of the amide ligand. For the ideal case of a planar amido ligand in a square–planar complex, considering N as a sp^2 center, the interaction between the Pd_{LUMO} (symmetric respect to the xz plane) and the $N_{lone\ pair}$ (antisymmetric respect the same plane) is symmetrically forbidden because the overlap is null (a in Fig. 4). When considering the Pd_{LUMO} in T-shaped complex, the overlap with the $N_{lone\ pair}$ becomes positive (b in Fig. 4). This positive overlap should further increase when considering the shape of the lone pair orbital in a pyramidal amide (c in Fig. 4). This last bonding interaction can be described as a single-face π interaction [2].

DFT molecular orbitals [70] were computed in our model complex $[PdPhNH_2PH_3]$. The HOMO is represented in Fig. 5. The existence of a single-face π interaction between the N of amido ligand and the Pd atom is clearly observed in the representation of the HOMO in Fig. 5. This kind of interaction is quite similar to the single-face π interaction proposed in Fig. 3c. The analysis of the HOMO for the complex with the largest amido ligand, $[PdPhN_tBu_2PH_3]$ provides a similar picture.

3.2.2 Electron density studies

The Pd–N bond was further analyzed in the frame of quantum theory of atoms in molecules (QTAIM) [62, 63]. Six model structures were used for this purpose: the simplest amido complex ($[PdPh(NH_2)(PH_3)]$), the related ammonia complex lacking lone pair to form double bond ($[PdPh(NH_3)(PH_3)]^+$), the complex with the largest amide ($[PdPh(N^tBu_2)(PH_3)]$); and a series of organic amines with different degrees of π delocalization over the C–N bond, namely methylamine (with no delocalization), aniline (with some delocalization), and formamide (highly delocalized).

A bond critical point (BCP) between N and Pd for organometallic complexes and between N and C for organic compounds was localized (Table 3). Electron density (ρ) at the BCP is directly related with the electronic population in the bond. The value of ρ in amido complexes is significantly higher than for the ammonia complex, indicating that in these complexes the bond is more electron populated. This may be attributed to some electronic contribution of the lone pair of the N atom to the Pd–N bond. Calculations in the organic molecules support this

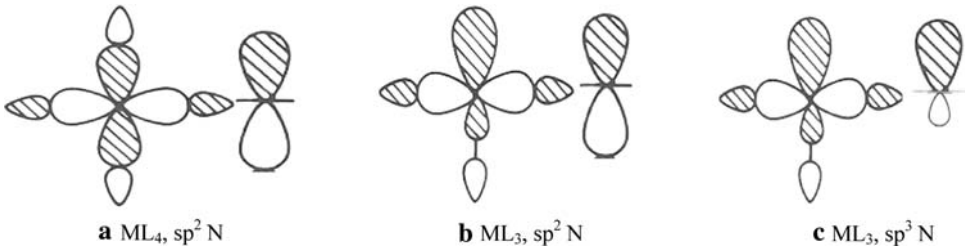

Fig. 4 Schematic representation of the interactions between the Pd LUMO and the N lone pair orbital in the ML_4 and ML_3 minima structures

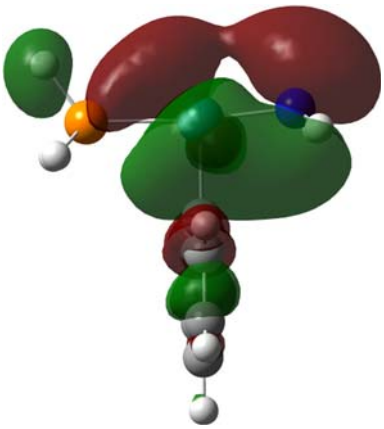

Fig. 5 The HOMO representation for the $[PdPhNH_2PH_3]$ complex

Table 3 Electron density analysis results in bond critical points, ε = ellipticity; ρ = electron density

Model	$\varepsilon_{(E-N)}$	$\rho_{(E-N)}$	$\varepsilon_{(Pd-P)}$	$\rho_{(Pd-P)}$
[Pd]–NH_2	0.072	0.133	0.086	0.087
[Pd]–N^tBu_2	0.072	0.119	0.054	0.096
[Pd]–NH_3^+	0.072	0.082	0.069	0.079
CH_3–NH_2	0.038	0.268		
Ph–NH_2	0.062	0.302		
HCO–NH_2	0.092	0.319		

interpretation and show an increase of electron density as the nitrogen lone pair delocalization raises.

Ellipticity is a property of the electron density that gives an idea of the anisotropy of the bond; low ellipticities are related with more cylindrical bonds. Because the electron density of π bonds is located up and down a nodal plane, double bonds usually have high ellipticities. In this case, no differences in ellipticity were obtained for any of the metal complexes. As far as organic molecules are concerned, the ellipticity values of the C–N bond increases when the character of double bond increases: 0.038 for Me–NH_2, 0.062 for Ph–NH_2 and 0.092 for HCO–NH_2. The value obtained for the Pd–N bond (0.072) is in the range of those obtained for organic compounds with a significant double bond character.

The Pd–N bond was also analyzed by means of the electron localization function (ELF). The analysis of the ELF is useful to understand the shape and behavior of electron density in a molecule. [71] This function uses the Pauli Exclusion Principle to evaluate the localization of electrons and to divide the total electron density in a set of basins centered in the electron pairs of the molecule. ELF analysis on Pd–N bond was performed in the model complexes $[Pd(Ph)(NH_2)(PH_3)]$ and $[Pd(Ph)(N^tBu_2)(PH_3)]$. Figure 6 shows the different basins obtained for these two complexes.

In both cases four different basins were identified in the electron density around N atoms. Two of them are defined as N–R (R = ^{t}Bu and H) bonding electron pairs by their position and shape. The other two are defined as lone pairs [72, 73]; their orientation is used to identify them as the dative and the proper lone pair. In the NH_2 model one of them is situated in the region between atoms (corresponding to the N–Palladium bonding interaction) and the other is situated over the N atom, near the position expected for a lone pair. The last one is distorted towards the N–Pd region. In the N^tBu_2 model complex, where T-shaped stabilization is higher, the lone pair basin is even more displaced towards the N–Pd region and, in fact, the other basin is displaced out of the bond line; both basins are highly symmetrically distributed around the N–Pd region, denoting a certain double bond character. The ELF function value at the point connecting both basins should be quite high, therefore hampering the drawing of both basins separately in Fig. 6. This suggests that there is a significant part of the electronic population in the region between both electronic pairs, suggesting delocalization between them.

Concerning the population of the basins, in the model amide ligand (NH_2) the global population around the N atom is of 7.43 electrons. Thus, 0.57 electrons from the amide ligand are delocalized throughout the complex. The basins corresponding to N–H have populations around two electrons (1.90 and 2.01 electrons). The basin located in the Pd–N region has 1.04 e, whereas the other basin has a population over the electron pair (2.48e). The complex with the largest amide (N^tBu_2) has a global electron population of 7.24e. Thus, 0.76 electrons from the amide ligand are delocalized throughout the system. The

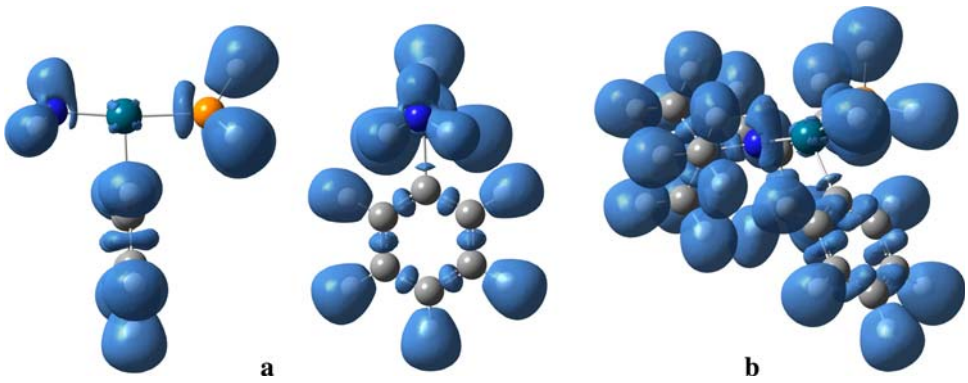

Fig. 6 Isosurfaces ELF = 0.80 of the model complexes: **a** [Pd(Ph)(NH_2)(PH_3)] (two views), and **b** [Pd(Ph)(N^tBu_2)(PH_3)]. N *blue*, Pd *green*, P *orange*, C *gray*

electronic population for both ^{t}Bu groups is 23.77e, compared to the theoretical value of 24e. Therefore, the electron is mainly delocalized over the metallic frame. The electronic population of the non-bonding basins in the Pd center is 8.79e. The two basins on the N–Pd are 2.13e and 1.58e.

Relative fluctuation (λ) is a parameter that can be calculated from ELF for each basin. A λ value higher than 0.45 is indicative of delocalization [74]. The values of λ calculated for some basins on the complex with the NH_2 amide are: 0.47 for basin of the lone pair on the N, 0.72 for the Pd–N basin, 0.67 for Pd–C bond, and 0.50 for Pd–P. All of the Pd–ligand bonds described by this method are as lone pairs over the ligand. The values obtained for λ suggest that all of these electron pairs are significantly delocalized over the metal. Importantly, a similar delocalization is also revealed for the lone pair of the N center. For the sake of comparison, the λ values obtained for the C–C bonds over the aromatic ring in the Ph ligands are between 0.47 and 0.48. For the complex with the N^tBu_2 amide the λ values of the basins around the Pd–N interaction are 0.53 and 0.63.

3.2.3 NBO analysis

Natural bond orbital (NBO) analysis was also performed for the complexes [Pd(Ph)(NR_2)(PH_3)] ($NR_2 = NH_2$, N^tBu_2) to analyze the N–Pd bond. To gain more insight into the description of the Pd–N bond, the NBO analysis over the simplest complex (amide = NH_2) was carried out with different geometries along the N–Pd bond rotation, that is the minimum, the transition state of rotation (rotated around 180°), and a constrained structure with the amido ligand rotated 90°. As we let NBO algorithm to describe the NBOs distribution along the whole complex, single bond structures (with just one bonding NBO between N and Pd centers) are proposed for all structures. Selected NBO parameters are compiled in Table 4.

According to the population in the bonding orbital, the electron density along the Pd–N bond decreases as the stability of the complex increases. This contradiction, along with the high population in the antibonding orbital suggests that the electronic distribution between bonding and antibonding NBO orbitals is not properly described. The antibonding population probably corresponds to some bonding extra-population that cannot be considered a second bonding orbital by NBO algorithm. This justification can be supported by the analysis of the aromatic ring, with the six electrons corresponding to the *p* cloud distributed in three bonding NBOs with 1.6–1.7 electrons and three antibonding NBOs with more than 0.3 electrons. As far as the lone pair population is concerned, it is lower in the minimum suggesting a higher delocalization than in the distorted geometries.

Furthermore, the whole proposed NBO distribution can be evaluated by considering the percentage of electronic population which is well defined by the Lewis structure (i.e. in lone pairs or bonding orbitals). The relative weight of this structure and the most similar one with a double N–Pd bond was studied by calculation of the NBOs constraining the

Table 4 Natural bond orbital results in different rotamers of [Pd(Ph)(NH_2)(PH_3)], pop = electronic population

Model	ΔE kcal/mol	Rot. angle [67] (°)	$Pop_{lone\ pair}$ n° e^-	$Pop^a_{bonding}$ n° e^-	$Pop^a_{antibonding}$ n° e^-	$Pop_{Lewis\ structure}$ %
Minimum	0.0	60.5	1.889	1.852	0.470	98.10
TS	10.3	−106.5	1.918	1.917	0.398	98.22
Perp.	8.8	−33.8	1.949	1.897	0.411	98.22

[a] Pd–N bond

Table 5 Natural bond orbital results in Lewis structure forced calculations of [Pd(Ph)(NH_2)(PH_3)] and [Pd(Ph)(N^tBu_2)(PH_3)], pop = electronic population

Model	$Pop_{lone\ pair}$ n° e^-	Pop^a_{bond1} n° e^-	Pop^a_{ant1} n° e^-	Pop^a_{bond2} n° e^-	Pop^a_{ant2} n° e^-	$Pop_{Lewisstructure}$ %
Pd–NH_2	1.683	1.949	0.434	–	–	96.54
Pd=NH_2	–	1.909	0.393	1.814	0.427	96.40
Pd–N^tBu_2	1.621	1.899	0.377	–	–	98.30
Pd=N^tBu_2	–	1.898	0.418	1.862	0.294	98.32

[a] Pd–N bond

Lewis structure of the complex for two models, with single N–Pd bond and with double N–Pd bond (Table 5).

According to the percentage of population described by the NBO distribution, both bonding schemes are equally acceptable (for both amide ligands considered). Consequently, both Lewis structures can be considered as resonant forms of the real complex.

When NBO analysis is performed in the bigger amido-complex [PdPh(N^tBu_2)(PH_3)], the default Lewis structure corresponds neither to a single bond nor to a double bond. In this case, default NBO analysis suggests that amide ligand acts as an ion with two lone pairs around the N atom. Similar behavior of the NBO computations is also usually observed when computing phosphines [75, 76]. With a forced single bond, electron population of the lone pair is lower when the largest amide ligand (N^tBu_2) complex is considered; this may be related to a greater delocalization of the N lone pair over the metal center. For the case where the double Pd–N bond situation is forced for the N^tBu_2 complex, a better representation of the second bond is obtained since the bonding population is larger and the antibonding population is lower than in the NH_2 model.

4 Conclusions

The analysis of a family of three-coordinated T-shaped Pd(II) complexes with stoichometry [Pd(NR_2)(Ph)(PH_3)] and four-coordinated related suggests that a great deal of the extra stabilization of T-shaped species that contain the amido ligand is due to an additional bonding interaction established between the Pd center and the lone pair of the N atom. This additional interaction increases for more electrodonating amido substituents.

This interaction may be described as a single-face π interaction of the lone pair of the amido ligand with an unoccupied *d* orbital of the metal. This interaction is non-symmetric, taking place mainly through the face where the lone pair is located, which is illustrated by examination of the HOMO of the T-shaped amido Pd(II) complexes using a molecular orbital analysis. This additional interaction is also supported by the high rotation barrier calculated for the complexed amido ligand. Furthermore, several theoretical schemes as QTAIM, ELF and NBO also indicate a high delocalization of the lone pair over the metal center, suggesting that there is an interaction between the N lone pair and the metal center. Importantly, this kind of ligands could be used to favor experimentally dissociative processes, because their ability to change the electron donation lets them to act as stabilizers of the complex when the coordination number is diminished.

Acknowledgments We thank the Spanish Ministerio de Ciencia e Innovación for financial support (Projects CTQ2007-67411/BQU, CTQ2005-09000-C02-01, CTQ2005-09000-CO2-02, ORFEO Consolider Ingenio-2010:CSD2007-00006 and INTECAT Consolider Ingenio-2010: CSD2006-0003) and the Junta de Castilla y León (GR169). The Spanish MEC is acknowledged for a fellowship to S. Moncho.

References

1. Albano VG, Natile G, Panunzi A (1994) Coord Chem Rev 133:67. doi:10.1016/0010-8545(94)80057-X
2. Alvarez S (1999) Coord Chem Rev 193–195:13. doi:10.1016/S0010-8545(99)00085-5
3. Dewar MJS, Olivella S, Rzepa HS (1978) J Am Chem Soc 100:5650. doi:10.1021/ja00486a013
4. Dewar MJS, Olivella S, Stewart JJP (1986) J Am Chem Soc 108:5771. doi:10.1021/ja00279a018
5. Bofill JM, Olivella S, Sole A, Anglada JM (1999) J Am Chem Soc 121:1337. doi:10.1021/ja981926y
6. Maseras F, Lledós A (eds) (2002) Computational modeling of homogeneous catalysis. Kluwer, Dordrecht
7. Ziegler T, Autschback J (2005) Chem Rev 105:2695
8. Casares JA, Espinet P, Salas G (2002) Chem Eur J 8:4843. doi:10.1002/1521-3765(20021104)8:21<4843::AID-CHEM4843>3.0.CO;2-I
9. Espinet P, Echavarren AM (2004) Angew Chem Int Ed 43:4704 and references therein
10. Phan NTS, Van Der Sluys M, Jones CW (2006) Adv Synth Catal 348:609. doi:10.1002/adsc.200505473 and references therein
11. Littke AF, Fu GC (1998) Angew Chem Int Ed 37:3387. doi:10.1002/(SICI)1521-3773(19981231)37:24<3387::AID-ANIE3387>3.0.CO;2-P and references therein
12. Litke AF, Fu GC (1999) J Org Chem 64:10. doi:10.1021/jo9820059
13. Litke AF, Fu GC (2001) J Am Chem Soc 123:6989. doi:10.1021/ja010988c

14. Nishiyama M, Yamamoto T, Koie Y (1998) Tetrahedron Lett 39:617. doi:10.1016/S0040-4039(97)10659-1
15. Yamamoto T, Nishiyama M, Koie Y (1998) Tetrahedron Lett 39:2367. doi:10.1016/S0040-4039(98)00202-0
16. Hartwig JF, Kawatsura M, Hauck SI, Shaughnessy KH, Alcazar-Roman LM (1999) J Org Chem 64:5575. doi:10.1021/jo990408i
17. Kuwano R, Utsunomiya M, Hartwig JF (2002) J Org Chem 67:6479. doi:10.1021/jo0258913
18. Litke AF, Fu GC (2002) Angew Chem Int Ed 41:4177. doi:10.1002/1521-3773(20021115)41:22<4176::AID-ANIE4176>3.0.CO;2-U
19. Cárdenas DJ (2003) Angew Chem Int Ed 42:384. doi:10.1002/anie.200390123 and references therein
20. Hartwig JF (1998) Angew Chem Int Ed 37:2046. doi:10.1002/(SICI)1521-3773(19980817)37:15<2046::AID-ANIE2046>3.0.CO;2-L
21. Yamashita M, Cuevas Vicario JV, Hartwig JF (2003) J Am Chem Soc 125:16347. doi:10.1021/ja037425g and references therein
22. Bei X, Turner HW, Weinberg WH, Guram AS (1999) J Org Chem 64:6797. doi:10.1021/jo990805t
23. Bei X, Uno T, Norris J, Turner HW, Weinberg WH, Guram AS, Petersen JL (1999) Organometallics 18:1840. doi:10.1021/om9900162
24. Li GY (2002) J Org Chem 67:3643. doi:10.1021/jo010983y
25. Li GY, Zheng G, Noonan AF (2001) J Org Chem 66:8677. doi:10.1021/jo010764c
26. Li GY (2001) Angew Chem Int Ed 40:1513. doi:10.1002/1521-3773(20010417)40:8<1513::AID-ANIE1513>3.0.CO;2-C
27. Zapf A, Ehrentraut A, Beller M (2000) Angew Chem Int Ed 39:4153. doi:10.1002/1521-3773(20001117)39:22<4153::AID-ANIE4153>3.0.CO;2-T
28. Liu S-Y, Choi MJ, Fu GC (2001) Chem Commun (Camb) 2408. doi:10.1039/b107888g
29. Urgaonkar S, Nagarajan M, Verkade JG (2002) Tetrahedron Lett 43:8921. doi:10.1016/S0040-4039(02)02189-5
30. Old DW, Wolfe JP, Buchwald SL (1998) J Am Chem Soc 120:9722. doi:10.1021/ja982250+
31. Wolfe JP, Buchwald SL (1999) Angew Chem Int Ed 38:2413. doi:10.1002/(SICI)1521-3773(19990816)38:16<2413::AID-ANIE2413>3.0.CO;2-H
32. Harris MC, Buchwald SL (2000) J Org Chem 65:5327. doi:10.1021/jo000674s
33. Gómez Andreu M, Zapf A, Beller M (2000) Chem Commun (Camb) 2475. doi:10.1039/b006791l
34. Menzel K, Fu GC (2003) J Am Chem Soc 125:3718. doi:10.1021/ja0344563
35. Littke AF, Schwarz L, Fu GC (2002) J Am Chem Soc 124:6343. doi:10.1021/ja020012f
36. Stambuli JP, Bühl M, Hartwig JF (2002) J Am Chem Soc 124:9346. doi:10.1021/ja0264394
37. Stambuli JP, Incarvito CD, Hartwig JF (2004) J Am Chem Soc 126:1184. doi:10.1021/ja037928m
38. Cámpora J, Gutiérrez-Puebla E, López JA, Monge A, Palma P, Del Río D, Carmona E (2001) Angew Chem Int Ed 40:781. doi:10.1002/1521-3773(20011001)40:19<3641::AID-ANIE3641>3.0.CO;2-9
39. Hay-Motherwell R, Wilkinson G, Sweet TKN, Hursthouse MB (1996) Polyhedron 15:3163. doi:10.1016/0277-5387(96)00056-3
40. Ingleson MJ, Mahon MF, Weller AS (2004) Chem Commun (Camb) 2398. doi:10.1039/b410846a
41. Mole L, Spencer JL, Carr N, Orpen AG (1991) Organometallics 10:49. doi:10.1021/om00047a026
42. Carr N, Mole L, Orpen AG, Spencer JL (1992) J Chem Soc, Dalton Trans 2653. doi:10.1039/dt9920002653
43. Baratta W, Stoccoro S, Doppiu A, Herdtweck E, Zucca A, Rigo P (2003) Angew Chem Int Ed 42:105. doi:10.1002/anie.200390035
44. Yared YW, Miles SL, Bau R, Reed CA (1977) J Am Chem Soc 99:7076. doi:10.1021/ja00463a059
45. Urtel H, Meier C, Eisenträger F, Rominger F, Joschek JP, Hofmann P (2001) Angew Chem Int Ed 40:781. doi:10.1002/1521-3773(20010216)40:4<781::AID-ANIE7810>3.0.CO;2-T
46. Yamashita M, Hartwig JF (2004) J Am Chem Soc 126:5344. doi:10.1021/ja0315107
47. Moncho S, Ujaque G, Lledós A, Espinet P (2008) Chem Eur J 14:8986. doi:10.1002/chem.200800423
48. Rossi AR, Hoffmann R (1975) Inorg Chem 14:365. doi:10.1021/ic50144a032
49. Palacios AA, Alemany P, Alvarez S (1999) Inorg Chem 38:707. doi:10.1021/ic980634v
50. Frisch MJ, Trucks GW, Schlegel HB, Scuseria GE, Robb MA, Cheeseman JR, Montgomery JA Jr, Vreven T, Kudin KN, Burant JC, Millam JM, Iyengar SS, Tomasi J, Barone V, Mennucci B, Cossi M, Scalmani G, Rega N, Petersson GA, Nakatsuji H, Hada M, Ehara M, Toyota K, Fukuda R, Hasegawa J Shida M, Nakajima T, Honda Y, Kitao O, Nakai H, Klene M, Li, Knox JE, Hratchian HP, Cross JB, Bakken V, Adamo C, Jaramillo J, Gomperts R, Stratmann RE, Yazyev O, Austin AJ, Cammi R, Pomelli C, Ochterski JW, Ayala PY, Morokuma K, Voth GA, Salvador P, Dannenberg JJ, Zakrzewski VG, Dapprich S, Daniels AD, Strain MC, Farkas O, Malick DK, Rabuck AD, Raghavachari K, Foresman JB, Ortiz JV, Cui Q, Baboul AG, Clifford S, Cioslowski J, Stefanov BB, Liu G, Liashenko A, Piskorz P, Komaromi I, Martin RL, Fox DJ, Keith T, Al-Laham MA, Peng CY, Nanayakkara A, Challacombe M, Gill, PMW, Johnson B, Chen W, Wong MW, Gonzalez C, Pople JA (2004) Gaussian 03, revision C.02. Gaussian Inc., Wallingford, CT
51. Perdew JP, Burke K, Wang Y (1996) Phys Rev B 54:16533. doi:10.1103/PhysRevB.54.16533
52. Becke AD (1993) J Phys Chem 98:648
53. Hay PJ, Wadt WR (1985) J Phys Chem 82:299. doi:10.1063/1.448975
54. Wadt WR, Hay PJ (1985) J Phys Chem 82:284. doi:10.1063/1.448800
55. Höllwarth A, Böhme M, Dapprich S, Ehlers AW, Gobbi A, Jonas V, Köhler KF, Stegman R, Veldkamp A, Frenking G (1993) Chem Phys Lett 208:237. doi:10.1016/0009-2614(93)89068-S
56. Cancès MT, Mennucci B, Tomasi J (1997) J Chem Phys 107:3032. doi:10.1063/1.474659
57. Cossi M, Barone V, Mennucci B, Tomasi (1998) J. Chem Phys Lett 286:253. doi:10.1016/S0009-2614(98)00106-7
58. Mennucci B, Tomasi J (1997) J Chem Phys 106:5151. doi:10.1063/1.473558
59. Cossi M, Scalmani G, Rega N, Barone V (2002) J Chem Phys 117:43. doi:10.1063/1.1480445
60. Braga AAC, Ujaque G, Maseras F (2006) Organometallics 25:3647. doi:10.1021/om060380i
61. Bo C, Ortiz JC Xaim 1.0, Universitat Rovira i Virgili, Tarragona
62. Bader RFW (1990) Atoms in molecules: a quantum theory. Oxford University Press, Oxford
63. Bader RFW (1991) Chem Rev 91:893. doi:10.1021/cr00005a013
64. Noury S, Krokidis X, Fuster F, Silvi B (1999) ToPMoD, Laboratoire de Chimie Théorique, Université Pierre et Marie Curie, Paris
65. Glendening ED, Badenhoop JK, Reed AE, Carpenter JE, Bohman JA, Morales C, Weindhold F (2001) NBO 5.0, Theoretical Chemistry Institute, University of Wisconsin, Madison
66. Dennington R II, Keith T, Millam J, Eppinnett K, Hovell WL, Gilliland R (2003) GaussView, Version 3.09, Semichem, Inc., Shawnee Mission
67. Dihedral HNPdC angles correspond to the dihedral angle between the plane defined by H, N and Pd, and the plane defined by N, Pd and the *ipso* C of the aromatic ligand

68. Albright T, Burdett JK, Whango MH (1985) Orbital interactions in chemistry. Willey, New York
69. Jean Y (2005) Molecular orbitals of transition metal complexes. Oxford University Press, Oxford
70. The shape and symmetry properties of the KS orbitals are very similar to those calculated by HF methods. See Stowasser R, Hoffmann R (1999) J Am Chem Soc 121:3414. doi:10.1021/ja9826892
71. Silvi B, Savin A (1994) Nature 371:683. doi:10.1038/371683a0
72. The identification of the dative N-Pd bond as a lone pair is not a consequence of the utilization of pseudopotentials for the Pd atom. Calculations performed with an all electrons basis set for the Pd center give the same identification of the electron pairs. The all-electron basis set employed was the Well-Tempered Gaussian Basis Set (WTBS). See Huzinaga S, Klobukowski M (1993) Chem Phys Lett 212:260. doi:10.1016/0009-2614(93)89323-A
73. Huzinaga S, Miguel B (1990) Chem Phys Lett 175:289. doi:10.1016/0009-2614(90)80112-Q
74. Llusar R, Beltrán A, Andrés J, Fuster F, Silvi B (2001) J Phys Chem A 105:9460. doi:10.1021/jp011906+
75. Maseras F, Morokuma K (1992) Chem Phys Lett 195:500. doi:10.1016/0009-2614(92)85551-K
76. Leyssens T, Peeters D, Orpen G, Harvey JN (2007) Organometallics 26:263. doi:10.1021/om061151z